

Boston University**OpenBU****<http://open.bu.edu>**

BU Open Access Articles

BU Open Access Articles

2014-02-14

Use of graphene as protection film in biological environments

*This work was made openly accessible by BU Faculty. Please [share](#) how this access benefits you.
Your story matters.*

Version	
Citation (published version):	Weixia Zhang, Sudarat Lee, Kelly L McNear, Ting Fung Chung, Seunghyun Lee, Kyunghoon Lee, Scott A Crist, Timothy L Ratliff, Zhaohui Zhong, Yong P Chen, Chen Yang. 2014. "Use of graphene as protection film in biological environments.." Sci Rep, Volume 4:4097.

<https://hdl.handle.net/2144/27000>

Boston University



OPEN

Use of graphene as protection film in biological environments

SUBJECT AREAS:

GRAPHENE
NANOBIOTECHNOLOGYWeixia Zhang¹, Sudarat Lee^{1*}, Kelly L. McNear¹, Ting Fung Chung^{2,3}, Seunghyun Lee⁴, Kyunghoon Lee⁴, Scott A. Crist^{5,6}, Timothy L. Ratliff^{5,6,7}, Zhaohui Zhong⁴, Yong P. Chen^{2,3,8} & Chen Yang^{1,2}Received
9 July 2013Accepted
28 January 2014Published
14 February 2014

¹Department of Chemistry, Purdue University, West Lafayette, Indiana 47907, United States, ²Department of Physics, Purdue University, West Lafayette, Indiana 47907, United States, ³Birck Nanotechnology Center, Purdue University, West Lafayette, IN, 47907, United States, ⁴Department of Electrical Engineering and Computer Science, University of Michigan, Ann Arbor, Michigan 48109, United States, ⁵Department of Comparative Pathobiology, Purdue University, West Lafayette, Indiana 47907, United States, ⁶The Center for Cancer Research, Purdue University, West Lafayette, Indiana 47907, United States, ⁷College of Veterinary Medicine, Purdue University, West Lafayette, Indiana 47907, United States, ⁸School of Electrical and Computer Engineering, Purdue University, West Lafayette, Indiana 47907, United States.

Correspondence and requests for materials should be addressed to C.Y. (yang@purdue.edu)

* Current address: Department of Chemistry, University of Michigan, Ann Arbor, Michigan 48109, United States.

Corrosion of metal in biomedical devices could cause serious health problems to patients. Currently ceramics coating materials used in metal implants can reduce corrosion to some extent with limitations. Here we proposed graphene as a biocompatible protective film for metal potentially for biomedical application. We confirmed graphene effectively inhibits Cu surface from corrosion in different biological aqueous environments. Results from cell viability tests suggested that graphene greatly eliminates the toxicity of Cu by inhibiting corrosion and reducing the concentration of Cu²⁺ ions produced. We demonstrated that additional thiol derivatives assembled on graphene coated Cu surface can prominently enhance durability of sole graphene protection limited by the defects in graphene film. We also demonstrated that graphene coating reduced the immune response to metal in a clinical setting for the first time through the lymphocyte transformation test. Finally, an animal experiment showed the effective protection of graphene to Cu under *in vivo* condition. Our results open up the potential for using graphene coating to protect metal surface in biomedical application.

Due to their strength and excellent resistance to fatigue degradation, metals are extensively used in medical fields such as bone and joint replacements^{1–3}, stents^{4,5}, dental materials^{6,7} and pacemaker cases or generators^{8,9}. For instance, stainless steels, pure titanium and titanium alloys, and cobalt-base alloys are the most common orthopaedic materials for total joint prostheses articulating with a plastic bearing surface for hips, knees, shoulders, ankles, and many others^{10,11}. In addition, dental amalgam alloys including mercury, silver, tin, and copper, and sometimes zinc, palladium, indium, selenium and recently titanium have been in use for restoring chewing surfaces^{12,13}. Despite of numerous successes, the main disadvantage of most metals or metal alloys used in medicine is that they corrode due to chemical reactions with the body enzymes and acids. It has been demonstrated by N. J. Hallab *et al.* that soluble metal ions produced during corrosion induces an innate monocytes/macrophage response and thus triggers immune responses, causing toxic, inflammatory and allergic or mutagenic reactions to patients¹⁴. Corrosion can also generate metallic debris, including metal particles and inorganic or organometallic compounds, which can deposit into the periprosthetic soft tissues to cause metallosis¹⁵. In addition to these adverse biological reactions, the corrosion process also degrades the structural integrity of metal devices, resulting in premature structural failure or loosening¹⁶. Therefore, how to protect metals from corrosion under physiological environment is a critical issue to be addressed for the sustainable biomedical application of metals.

Corrosion is a gradual destruction of materials caused by various interactions between the materials and the environment. Specifically, biological corrosion occurring in complex aqueous environment is mainly due to electrochemical processes. The basic underlying reaction during biological corrosion is that, when contacting to biological environment, metals are oxidized through electrochemical reactions to form ions, which then may result in formation of soluble or insoluble metallic products or migrating away from the metal surface as free ions¹⁷. To inhibit the corrosion process, protective coatings can be used to isolate metals from the environment, such as body fluids. For example, zirconia ceramic surface transitioned from zirconium alloy is able to greatly minimize corrosion and has been used in knee implants since 2001^{18–20}. However, it deteriorates and roughens as it ages. A group of nanodiamond coating, including diamond-carbon coating and apatite-nanodiamond

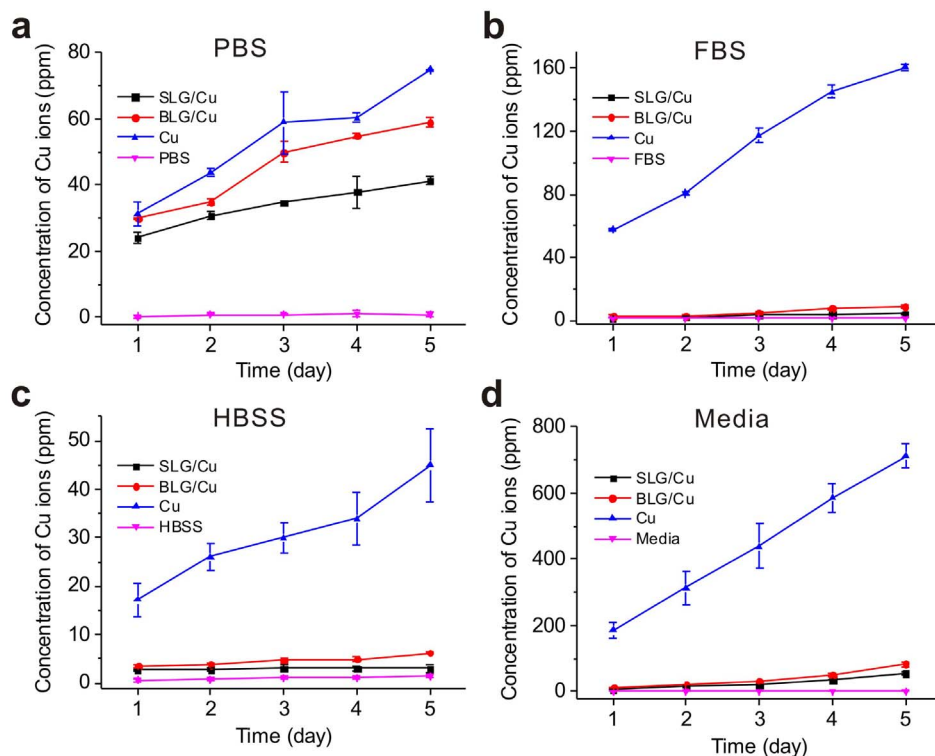


Figure 1 | Concentration of Cu^{2+} ions from different biological solutions. Concentrations of Cu^{2+} ions in (a) PBS, (b) FBS, (c) HBSS solutions and (d) cell culture media with presence of SLG/Cu (black), BLG/Cu (red) and Cu (Blue) and blank solutions as controls (Pink) measured by ICP-MS, respectively. All results are presented in a mass ratio (ppm).

composite coatings^{21,22}, recently has been proposed to hinder corrosion for metal implants. However, noticeable permeability and rough coating surface deteriorate their performance.

Recent advances in graphene research open up its great potential in suppressing metal corrosion in biological systems. Graphene, a flat atomic monolayer composed of sp^2 -bonded carbon atoms, has been shown as a promising biocompatible scaffold²³. Additionally, graphene is chemically inert and impermeable to gases even helium^{24,25}. J. Cho *et al.* and J. Park, R. S. Ruoff *et al.* have demonstrated that graphene can provide effective oxidation resistance for the underlying Cu and Cu/Ni alloys^{25,26}. Large scale synthesis of high quality and uniform graphene films could be achieved through chemical vapor deposition (CVD) method²⁷. All these remarkable characteristics enable graphene to be considered as an excellent protective coating candidate for metals. K. I. Bolotin *et al.* and N. Birbilis *et al.* have demonstrated that graphene films could serve as corrosion-inhibiting coatings and have studied the passivation mechanism using electrochemical techniques^{28,29}, respectively. Recently, F. Alexis and A. Rao *et al.* have reported that graphene coating could enhance both bio- and hemo-compatibility of implant materials^{30,31}. Notably, it has been found that in F. Alexis and A. Rao's study, almost all the cell viability results with the presence of graphene coated NiTi were compatible or even lower than those observed for pristine NiTi, indicating a modest protection offered by graphene to NiTi if there was any. In this work, we demonstrate the potential of graphene as a biocompatible protection film *in vitro* and, for the first time, *in vivo*. In our work, we chose Cu, a less biocompatible metal than NiTi, partially because it is the catalyst for graphene synthesis, more importantly, it is one of the most toxic heavy metals³², therefore it can offer a more sensitive system for cell viability and metal sensitivity tests. In addition to cell viability experiment, we carried out for the first time lymphocyte transformation test (LTT), a standard clinical test, to demonstrate that graphene coating can reduce immune response. More significantly, we performed the first *in vivo* experiments

studying protection of Cu by graphene in live animals to evaluate the potential of using graphene as a biocompatible passivated coating for metals in physiological conditions. Chemically, we explored a new strategy to utilize additional thiol derivatives self-assembled on metal surface to effectively enhance the durability of graphene protection. Our results indicated graphene coating could successfully protect metals and inhibit their corrosion in biological environments.

Results

Single layer graphene (SLG) used in this study was grown on 25 μm thick Cu foils using chemical vapor deposition (CVD) conducted under atmospheric pressure as previously reported³³. Graphene was expected to be synthesized on both sides of the Cu foils.

The protection effect of graphene on Cu foils in the aqueous environment was first confirmed through monitoring corrosion of Cu chemically. The corrosion of as-synthesized SLG coated Cu foils (labeled "SLG/Cu") and bare Cu foils (labeled "Cu") in phosphate buffered saline (PBS), fetal bovine serum (FBS), hank's balanced salt solution (HBSS), and cell culture media were tested. Corrosion of Cu was monitored through measuring the concentrations of Cu^{2+} ions, the primarily corrosion products generated by the reaction of Cu with these solutions³⁴, using inductively coupled plasma-mass spectrometry (ICP-MS) on day 1, 2, 3, 4 and 5. All samples were measured in triplicate. Results are shown in Fig. 1.

For all solutions tested, ICP-MS results clearly confirmed that concentrations of Cu^{2+} ions obtained for SLG protected Cu samples (black) were always lower than those of bare Cu samples (blue) at all time periods measured. Over time, Cu^{2+} ion concentrations measured for SLG/Cu and Cu samples both increased as a cumulative result of the corrosion. Additionally, variation in Cu^{2+} ion concentrations measured from the bare Cu samples for these solutions indicated different etching ability of the solutions, with cell culture media as the most corrosive one and HBSS the weakest one. Besides, in FBS, HBSS and media, graphene coating in SLG/Cu substantially



reduced the concentrations of Cu^{2+} ions compared to the corresponding concentration from bare Cu. Distinctively, in PBS, Cu^{2+} ion concentration measured from SLG/Cu seemed much closer to that measured from the bare Cu samples. We attributed this result to the formation of low soluble copper phosphate in PBS. Passivation of copper phosphate precipitates on the bare Cu surface effectively inhibited further etching of Cu, resulting in an apparent smaller Cu^{2+} ion concentration detected for bare Cu samples. At last, Cu^{2+} ions detected in the control (pink) were approximately zero, consistent with the composition of these biological solutions. Collectively, slower and less corrosion of Cu observed with the coating of graphene suggests that SLG successfully protects underlying Cu foils and hinder corrosion in these solutions.

We further tested the protection of bilayer graphene (BLG) with initial hypothesis that BLG potentially offers better protection based on additional graphene coverage on Cu surface. As-synthesized high-quality BLG coated Cu (labeled “BLG/Cu”), with over 99% bilayer coverage and a low defect density comparable to SLG³⁵, was used. Fig. 1 shows that for all solutions the Cu^{2+} ion concentration detected in the solution with BLG/Cu samples was lower than that of bare Cu sample over the testing periods as expected. Interestingly, the Cu^{2+} ion concentrations for BLG/Cu sample were found to be higher compared to those for the SLG/Cu sample in all solutions despite the fact that more carbon coverage offered by BLG. This result might be explained by stronger adhesion of SLG to Cu surface than that of BLG, benefiting from the better ability of SLG to adapt to the topography of the surface as a result of its flexibility, as indicated by J. S. Bunch *et al.*³⁶. BLG with weaker adhesion to Cu surface showed noticeably weaker protection effect compared with the SLG case. Collectively, our chemical experiments in different biological solutions confirmed that SLG and BLG coatings both inhibit the corrosion of Cu surface underlying, resulting in reduced concentration of Cu^{2+} ions, substantial amount of which could be fatal to cells. Impact of metal protection of SLG/Cu and BLG/Cu were then further evaluated in the following *in vitro* cell experiment.

MG-63 human bone cell line (American Type Culture Collection, ATCC, Rockville, MD, USA) was chosen for *in vitro* experiments, for its relevance when considering potential applications of graphene in metal joint implants. Despite the dose dependent *in vitro* toxicity of pristine graphene reported, graphene as a substrate has demonstrated to be favorable for the adhesion, proliferation, and differentiation of certain stem cells³². In our work, we first evaluated the effect of graphene as a substrate to MG-63 cell growth by testing cell viability of cultured MG-63 cells on SLG coated glass substrates in comparison to cell cultures on bare glass substrates. We found no differences in viability and cell morphology (See Supplementary Fig. S2). The negligible effect of graphene substrates for cell viability or cell growth was also observed by us in HeLa cell cultures previously. These results suggest that graphene is biocompatible when being considered for a protection film in biomedical application.

To evaluate the protection effect of graphene, we performed cell viability tests using graphene coated Cu as a toxic source in the MG-63 cell culture. After seeding cell suspension in cell culture plates, sterilized SLG/Cu, BLG/Cu foils and Cu foil with the identical sizes were added to individual wells. A regular culture in a well untreated with any foils was used as the control. Cellular experiments for each sample were conducted in triplicate. After incubation for 1 day, A metabolic activity assay, 3-(4, 5-dimethylthiazol-2-yl)-2, 5-diphenyltetrazolium bromide (MTT) was performed to assess the cell viability of each well. Cell viability data was normalized to what is measured for the control. Testing the cytotoxicity of Cu^{2+} ions intentionally delivered into cells was not in the scope of this study. A typical set of results is illustrated in Fig. 2. After incubation for 1 day the well with SLG/Cu sample shows $100.4\% \pm 2.2\%$ cell viability, identical to the control, and the cell viability measured for the BLG/Cu sample is

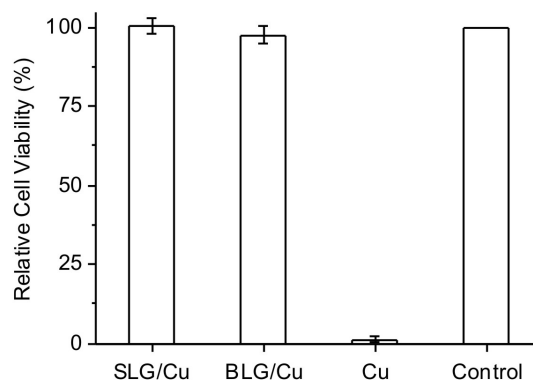


Figure 2 | Relative cell viability of bone cells incubated with SLG/Cu, BLG/Cu and bare Cu foil for 1 day. Control is the regular cell culture without presence of any Cu foil.

$97.6\% \pm 2.8\%$. In contrast, the cell viability for the well with Cu foil is approximately zero.

To confirm that such greatly improved cell viability is a result of inhibition of corrosion, we carried out ICP-MS measurements to detect the ion concentration in medium from each well. Fig. 3a shows Cu^{2+} ion concentrations measured from different sample wells. The highest to lowest concentrations were detected from medium in cell cultures with Cu (162.3 ± 25.8 ppm), BLG/Cu (22.1 ± 2.2 ppm), SLG/Cu (6.9 ± 0.3 ppm) and the control (0.6 ± 0.0 ppm), directly correlated to the lowest to highest cell viability detected from Cu, BLG/Cu, SLG/Cu and control samples (Fig. 2), respectively. Notably, despite that Cu^{2+} ion concentration inside the cells might be distinct from the concentration in the medium, fewer cells are expected to survive when exposed to higher concentration of Cu^{2+} ions. Additionally, the ionic concentration obtained from BLG/Cu culture is slightly larger than that from SLG/Cu culture, which is consistent with results of cell viability (Fig. 2) and chemical experiments (Fig. 1).

We also characterized the morphology of all sample surfaces used in the cellular experiments to directly visualize the impact of corrosion to the metal surface. Scanning Electron Microscopy (SEM) images in Fig. 3b exhibit surface morphology of SLG/Cu, BLG/Cu and Cu before and after incubation. Before incubation surfaces for all three samples were smooth. Contrast observed in images taken from as-synthesized SLG/Cu and BLG/Cu indicates defects of the graphene film and the exposed grain of the Cu foil. After incubation of 1 day, the surface of bare Cu became extremely rough due to the strong etching ability of medium to Cu. For both SLG and BLG surface, a noticeable graphene film remains on the surface after incubation (also See Supplementary Fig. S3). The surface of the Cu foil protected by graphene become rougher yet still much smoother compared to the bare Cu case.

In order to understand the durability of graphene protection, cell viability experiments were carried out with incubation time up to 4 days, which is longest incubation time limited by the life of the medium for the cell culture. Relative cell viability over 4 days is shown in Fig. 4a for each sample. Zero cell viability was again observed when the cell culture was exposed to bare Cu foil starting as early as 1 day. In the first two days, coating of SLG and BLG both successfully improved the cell viability compared to bare Cu foil, consistent with results shown in Fig. 2. Significantly, a substantial decrease in cell viability was observed at day 4 for both graphene coated samples, suggesting the cell viability is not linearly correlated to the exposure time period to Cu at day 4. Previous biometal toxicity studies have reported that the cell viability can decrease exponentially under the following scenarios. First, for the case of a constant ion concentration present in the medium incubation time exceeds a threshold exposure time, and second, for the case of a fixed incubation time considered the ion concentration exceeds a thresh-

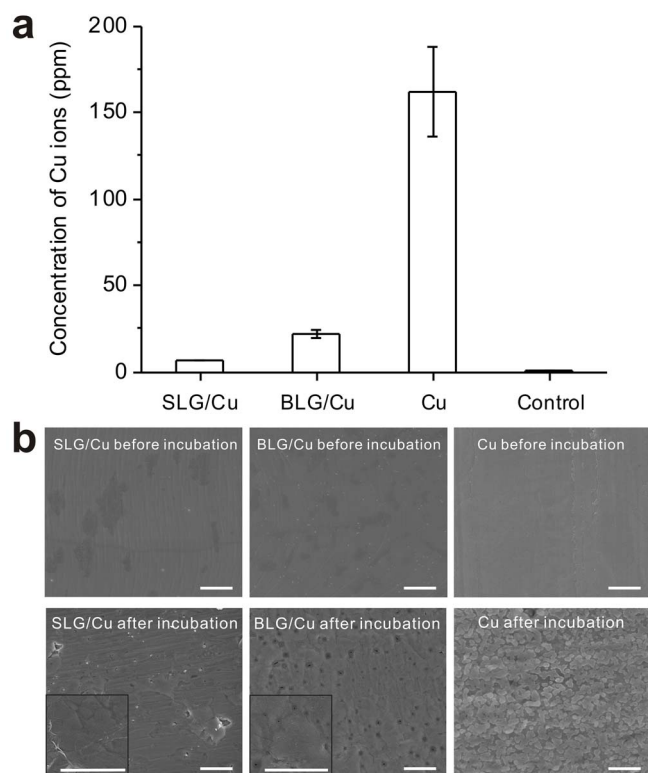


Figure 3 | Concentration of Cu ions and SEM images of Cu foils after incubation for 1 day. (a) Concentrations of Cu^{2+} ions of control medium, and of medium after incubated with SLG/Cu, BLG/Cu and Cu for 1 day. (b) SEM images of SLG/Cu, BLG/Cu and Cu before and after incubation. Insets are high magnification SEM images for SLG/Cu and BLG/Cu after incubation, respectively. Scale bar: 1 μm .

old concentration, often in the range of 1 ppm to 100 ppm for $\text{Cu}^{34,37,38}$. The non-linear decrease when incubation time was 3–4 days observed in our study is a result of increasing Cu^{2+} ion concentration over time, which is consistent with previous biometal studies.

We also measured the ion concentration in the media from cell cultures over time (Fig. 4b) and confirmed an increase in the ion concentration over time, directly correlated to the trend of cell viability for SLG/Cu and BLG/Cu samples. Significantly, increase in concentration of Cu^{2+} ion for SLG/Cu is reasonably linear (Fig. 4b), indicating that the non-linear decrease of cell viability observed from Fig. 4a cannot be attributed to the degradation of graphene.

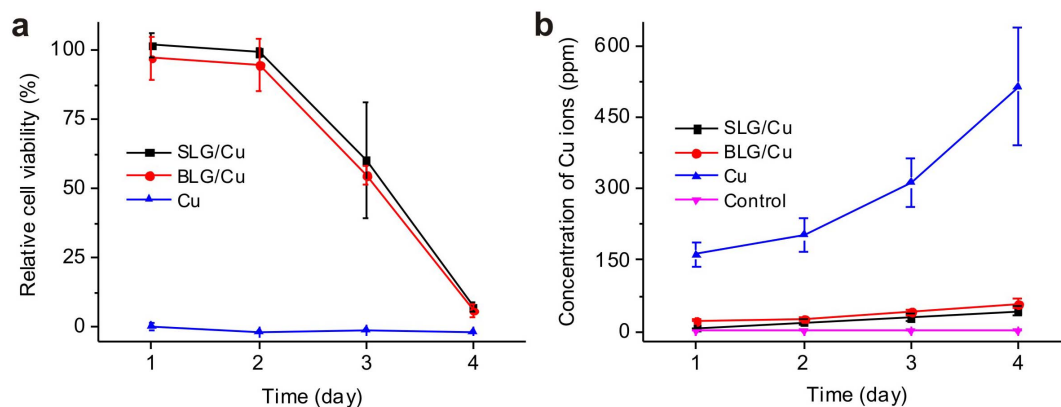


Figure 4 | Relative cell viability and concentration of Cu^{2+} ions as a function of time. (a) Relative cell viability vs. time for SLG/Cu, BLG/Cu and Cu samples; (b) Concentration of Cu^{2+} ions in cell culture medium after incubation with SLG/Cu, BLG/Cu and Cu samples calculated from ICP-MS. Medium taken from a regular cell culture without presence of any Cu foils is used as the control.

Noticeably, the concentration of Cu^{2+} ions for bare Cu measured in the medium from cell cultures (blue in Fig. 4b) is found to increase non-linearly with time, while Cu^{2+} ion concentration measured from the medium without presence of cells shows a linear increase over the same incubation period (Fig. 1d). This difference could be probably attributed to that for a relatively long incubation time, in this case, 3–4 days, an acidification induced by a sufficient amount of dead cells^{39,40} accelerates etching rate of Cu with presence of the cell culture, resulting in a higher Cu^{2+} ion concentration.

Ideally, a defect-free graphene can potentially offer effective long term protection by eliminating Cu^{2+} ion concentration. When defects exist, the corrosive solution diffuses through cracks of graphene resulting in local etching of Cu foil which are not only limited to the defects but may also progresses underneath the graphene film⁴¹. Overtime, the accumulative ion concentration exceeds toxicity limit and triggers the exponential decrease in cell viability. In this study, we explored the possibility of using metal surface functionalization to achieve more enduring protection^{42,43}. Here, we chose 1-Decanethiol to form self-assembly monolayer on Cu foil. Aliphatic thiols are specifically toxic to erythrocytes, and the toxicity decreases with increased chain length⁴⁴, so 1-Decanethiol with long chain length presents minimal cytotoxicity to bone cells used here. We expected that monolayer of 1-Decanethiol self-assembled on exposed Cu where graphene defects locate slows down the diffusion rate of medium because of hydrophobicity of alkyl chain and therefore improves protection.

As-synthesized SLG/Cu was cleaned and treated with ethanolic solution of the thiol⁴⁵ (labeled as “SLG/Cu-SH”). A piece of bare Cu foil with the identical size was also treated with thiol modification (labeled “Cu-SH”). Both SLG/Cu-SH and Cu-SH as well as unmodified SLG/Cu from the same growth batch, bare Cu were used for cellular experiments. After incubation for 3 days, MTT assay was performed to assess the cell viability. Results are showed in Fig. 5.

Compared to SLG/Cu, SLG/Cu-SH with thiol group protection exhibited improved cell viability from $26.5\% \pm 9.4\%$ to $55.8\% \pm 8.4\%$ at incubation of 3 days, while thiol coating in Cu-SH improved the viability to $1.9\% \pm 0.5\%$ compared to the $0.5\% \pm 1.5\%$ viability observed for bare Cu. Collectively, results suggested that SLG on Cu foil was the major factor for protection, and combined with additional thiol coating it offers an enhanced protection in a longer incubation period.

To extend the application of graphene coating, we also tested the performance of mechanically transferred graphene for inhibiting corrosion of metal surface. To establish a meaningful comparison between protections by as-grown graphene on Cu substrate and by transferred graphene on the same metal, SLG grown on Cu foil was

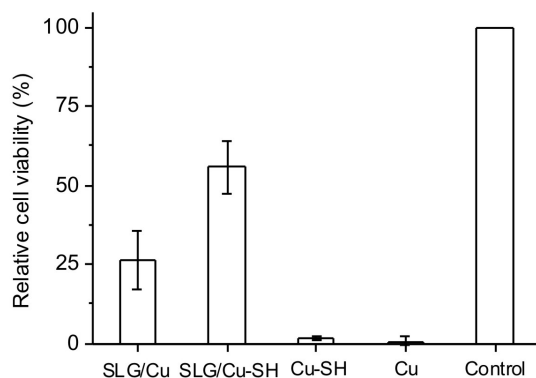


Figure 5 | Relative cell viability data of bone cells incubated with SLG/Cu, SLG/Cu-SH, Cu-SH and bare Cu foil for 3 days. Control is a regular cell culture without presence of any Cu samples.

transferred to another bare Cu foil (labeled “Tr-SLG/Cu”) following the typical transferring procedure reported^{28,33,35}. Additional thiol coating was also performed to the transferred sample (labeled “Tr-SLG/Cu-SH”) using the same strategy discussed above. Together with Cu and Cu-SH, Tr-SLG/Cu and Tr-SLG/Cu-SH were tested for cellular experiments. As shown in Fig. 6, cell viability obtained after 1 day incubation for the Tr-SLG/Cu sample is found to be $6.4\% \pm 3.9\%$, comparable with that obtained from Cu-SH and Cu, which is likely a result of tears and rips in the graphene film produced during its transfer²⁸. Transferred graphene, combined with additional thiol coating, offers reasonably well protection for Cu corrosion, resulting in $61.1\% \pm 6.2\%$ viability. These results suggested that although it provides limited protection, transferred SLG together with additional metal surface functionalization with thiol is possible to be considered as a universal protection film preventing metal corrosion in chemical, biological and medical applications.

To demonstrate that the effective protection offered by graphene coating for metal from corrosion further reduces the immune response of patients to metal potentially in biomedical application, we conducted the lymphocyte transformation test (LTT) with SLG coated Cu, bare Cu, Cu^{2+} ion solution in medium and standard negative and positive controls. LTT measures the proliferation of lymphocytes as a measure of immune response when lymphocytes have been exposed to potential toxic agents. It is the standard test proposed by the International Union of Immunological Societies to detect patient’s immune response to metal and commonly performed in the clinic setting before metal implant procedures^{46–48}.

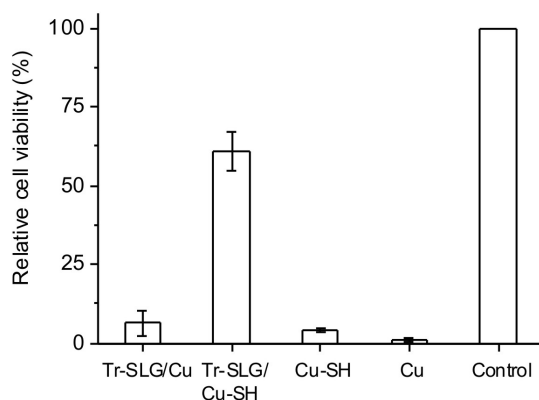


Figure 6 | Relative cell viability of bone cells incubated with Tr-SLG/Cu, bare Cu, Tr-SLG/Cu-SH, and Cu-SH for 1 day incubation. Control is a regular cell culture without presence of any Cu sample.

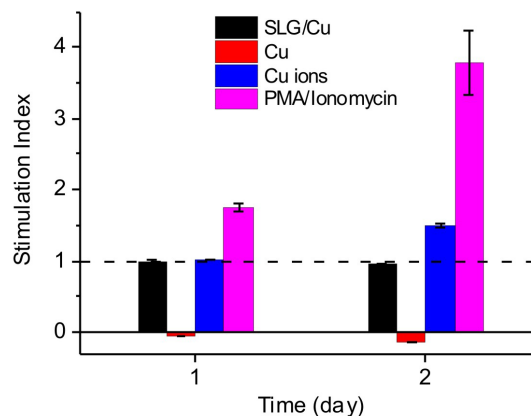


Figure 7 | Stimulation index for lymphocyte. After incubating with SLG/Cu (black), Cu foil (red), Cu^{2+} ions (blue) and PMA/Ionomycin (violet) for 1 day and 2 days.

In our work, LTT tests were performed for SLG/Cu and bare Cu samples. 6.6×10^{-3} mM Cu^{2+} ion solution in media was tested as a positive control considering Cu^{2+} ion as a toxic source activating lymphocytes. Combination of Phorbol-12-Myristate-13-Acetate (PMA) (25 ng/ml) and ionomycin (2.5 $\mu\text{g}/\text{ml}$) stimulating lymphocytes proliferation were used as another standard positive control. Untreated wells with lymphocytes culture were used as negative controls⁴⁹. The proliferations of lymphocytes for all samples were quantified by MTT⁵⁰. Stimulation index (SI), defined as the ratio of the absorbance of the sample detected in MTT tests to the absorbance of the negative control, is a measure of the lymphocytes proliferation and presented in Fig. 7. All samples were measured in triplicate.

Fig. 7 shows that the SIs for SLG/Cu samples were 0.99 ± 0.02 and 0.95 ± 0.01 after incubation for 1 day and 2 days, respectively, indicating that SLG/Cu does not activate lymphocyte proliferation. For bare Cu, after 1 day incubation the SI was -0.04 ± 0.001 , indicating that all cells were dead. Previously J. J. Jacobs and co-workers found that Cu^{2+} ion decreased lymphocyte proliferation to a SI lower than 0.5 at a concentration of 0.1 mM in the LTT experiment⁵¹. In our case, the Cu^{2+} ion concentration in the media for bare Cu samples was measured to be approximately 130 ppm or 2 mM, therefore a close to 0 SI found in our experiment was expected. It has been suggested that lower concentrations than 0.1 mM would be appropriate for metal-reactivity testing of Cu using LTT. Here we also chose a Cu^{2+} ion solution in medium with 6.6×10^{-3} mM for comparison. After 1 day and 2 day incubations, the SI obtained from the 6.6×10^{-3} mM Cu^{2+} ion solution was 1.01 ± 0.01 and 1.50 ± 0.03 , respectively, clearly indicating activation of lymphocytes. Lastly, the lymphocytes showed expected proliferation responses to PMA/Ionomycin, the standard positive control. The SIs measured were 1.76 ± 0.07 and 3.77 ± 0.45 for 1 day and 2 day incubations, respectively. Collectively, the LTT results, specifically the comparison of results from SLG coated Cu, Cu and 6.6×10^{-3} mM Cu^{2+} ion solution, demonstrated that protection effect of graphene preventing metal corrosion can substantially reduce immune response in a biological environment, opening potential to use graphene coating to improve metal devices for biomedical application.

At last, we performed an animal experiment to test the effect of graphene protection *in vivo* by surgically implanting graphene coated Cu foils and bare Cu foils into rats, respectively. Blood were extracted from implanted rats and the concentrations of Cu^{2+} ions were analyzed using ICP-MS. Blood samples from rats before implantation were used as control. Results, shown in Fig. 8, demonstrated the following key features. First, concentrations of Cu^{2+} ions in blood from rats with implanted SLG/Cu and bare Cu were both observed to increase with time. Second, we noticed that within 1 day

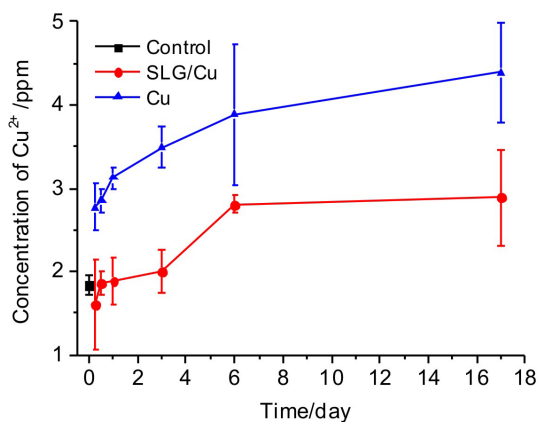


Figure 8 | Concentrations of Cu^{2+} ions in blood extracted from live rats. Concentrations of Cu^{2+} ions from normal rats before implantation as control (black square), rats with implanted SLG/Cu foils (blue triangles) and rats with implanted Cu foils (red dots) as a function of time after implantation.

after implantation, the concentrations of Cu^{2+} ions in blood of rats with SLG/Cu foils were close to those of control, while even just at 6 h after implantation, the concentrations of Cu^{2+} ions from rats with implanted bare Cu foils appeared to be more than 1.5 times of those of control. More significantly, the concentration of Cu^{2+} ions from rats with bare Cu foil were always detected to be higher than those from rats with SLG/Cu foils during the whole course up to 17 days after implantation. In summary, our results clearly demonstrated the protection effect of SLG can effectively inhibit corrosion of Cu therefore decrease concentration of Cu^{2+} ions under *in vivo* condition. It has been well studied that accumulated Cu^{2+} ions in blood results in undesirable biological effects, such as reducing organ function or leading to early death^{52,53}. Further investigation on impact of graphene protection on these adverse effects *in vivo* is needed.

Discussion

In summary, we explored the possibility of using graphene as a protective layer to inhibit corrosion of Cu foils in biological environment. Both chemical experiments and cellular experiments showed that SLG and BLG protection could both greatly minimize the concentration of Cu^{2+} ions, and therefore graphene coating substantially decrease the toxicity of Cu surface to bone cells, particularly in 1–2 day testing period. However, cumulatively increased ion concentration resulted from defects of graphene will trigger an exponential decrease in cell viability at day 3 and 4, which deteriorate enduring protection of graphene. Additional surface functionalization of thiol derivatives on graphene coated Cu foil has potential to significantly improve the durability of protection by hindering diffusion of medium through defects of graphene. Transferred graphene sheet offers reasonable protection when thiol functionalization was introduced. The LTT results indicate the graphene coating inhibits metallic allergic immune response. The animal study shows the graphene film can also provide effective protection to metals under *in vivo* condition. Our work demonstrated graphene coating could be used as a possible versatile strategy to protect metals under physiological conditions, opening up potentials for its biomedical application such as metal implants. For practical application of graphene in metal implants, as grown graphene on metals other than Cu needs to be developed and evaluated. Alternatively, further functionalization of graphene or metal might be possible to increase the interaction between graphene and Cu foil surface therefore enhance the protection of transferred graphene.

Methods

Graphene synthesis. SLG samples were grown on 25 μm thick of Cu foils (Sigma-Aldrich, 99.98%) by CVD at ambient pressure. The Cu foil was loaded into a CVD furnace and heated to 1000°C in 50 sccm of flowing H_2 . After 1000°C was attained, the foil was annealed for 1 hour. Then 10 sccm CH_4 was flowed for 30 min. The system was then cooled to room temperature.

To prepared BLG samples, the system was purged with argon gas and evacuated to a vacuum of 0.1 Torr after loading Cu foil into furnace. The foil was then heated to 1000°C in 100 sccm H_2 environment at 0.35 Torr. When 1000°C was reached, 70 sccm of CH_4 was flowed for 15 min at 0.45 Torr. The sample was then cooled slowly to room temperature at a rate of 18°C/min. The pressure was maintained at 0.5 Torr with 100 sccm of argon flowing during cooling.

Raman spectroscopy was performed on graphene transferred on SiO_2/Si substrates with laser excitation wavelength of 514 nm. The spectra (See supplementary Fig. S1) showed single-layer and bilayer features for SLG and BLG, respectively.

Chemical experiment. As-synthesized SLG/Cu, BLG/Cu and bare Cu with the identical size of 1.2 cm \times 1.2 cm were cleaned with acetone and isopropanol and then immersed in 3 ml of different biological solutions, including PBS, FBS, HBSS and cell culture media. Solutions without the presence of Cu were used as the control for each group receptively. All samples were placed in an oven at 37°C. For FBS, HBSS and cell media samples, 200 μl of solution was taken and diluted with ultra-pure water and 70% nitric acid (VWR, Aristar Ultra) to 10 ml. For PBS samples, due to precipitation of insoluble copper phosphate, sample solutions were first sonicated to get uniform suspension, and then 200 μl of the suspension were taken and diluted with ultrapure water and 70% nitric acid to 10 ml. All diluted solutions were allowed to statically stand for 24 hours to achieve homogenous solutions. Afterwards, 200 μl of the diluted solution was further diluted with 2% nitric acid to 10 ml, and then analyzed by ICP-MS. A Cu^{2+} ion solution of 10 ppb weight to weight ratio was used as the standard.

Cellular experiment. MG-63 human bone cell line (American Type Culture Collection, ATCC, Rockville, MD, USA) was used. In a typical experiment, 3 ml of cell suspension with density of 1×10^5 cells/ml were added into each well of a 6-well plate, and first incubated with a TCC-formulated Eagle's Minimum Essential Medium for 4 hours allowing cells to adhere to the bottom of the well. Then sterilized SLG/Cu, BLG/Cu foils and Cu foil with the identical sizes were added to individual wells. A regular culture in a well untreated with any foils was used as the control. The plate was then transferred into an incubator at 37°C with a humidified atmosphere containing 5% CO_2 . After incubation for 1 day, the cell culture medium and all Cu foils were gently removed from wells and wells were washed twice with 1 ml PBS solution. Then a metabolic activity assay, 3-(4, 5-dimethylthiazol-2-yl)-2, 5-diphenyltetrazolium bromide (MTT) was performed to assess the cell viability of each well. Cell viability data was normalized to what is measured for the control. 200 μl of cell culture medium removed from wells before MTT tests was used for ICP-MS measurement. For long term incubation, instead of changing media every other day³⁰, we kept the same media in each well during the cell viability experiment, considering the cytotoxicity of metals mainly relies on accumulated concentration of metal ions. Maintaining media over the test course offered a more meaningful result to evaluate graphene protection.

Thiol functionalization. As-synthesized SLG/Cu was quickly treated with hydrochloric acid to remove oxide layer, then rinsed with ultrapure water to remove residual impurities. After being dried in nitrogen, the SLG/Cu foil was immediately immersed in a 7.5 mM ethanolic solution of the thiol. After 2 h in the thiol solution the sample (labeled "SLG/Cu-SH") was copiously rinsed with ethanol to remove the physisorbed material and finally dried with nitrogen.

Graphene transfer. To transfer graphene to another substrate, one side of the as-synthesized SLG was coated with PMMA (Microchem) resist and cured at 180°C for 1 min. The other side of the sample was exposed to O_2 plasma to remove the graphene on that side. The sample was then left in Ammonium persulfate (VWR, 98%) solution for overnight to completely dissolve away the copper layer. Then the graphene was transferred to one side of a Cu foil with almost the same size. The process was repeated to transfer another piece of graphene to the other side of the Cu foil. The PMMA coating was removed with acetone and isopropanol. Finally, the Cu foil was rinsed with deionized water several times.

Lymphocyte transformation test. Mouse spleen tissues were collected aseptically and subsequently transferred to a sterile Petri dish containing medium. The spleen tissues were then grounded to release cells to medium. After centrifuging the cell suspension, the supernate was removed, and the precipitate was treated with Ammonium-Chloride-Potassium (ACK) for a few minutes to lyse the present red blood cells. Then PBS was added and the solution was centrifuged again to collect the lymphocyte precipitate. Lymphocytes suspension with a density of 5×10^6 cells/ml was then prepared by mixing the lymphocyte precipitate with RPMI 1640 medium. 3 ml of the lymphocytes suspension were added into each well of a 6-well plate. Then 1.0 cm \times 1.0 cm SLG/Cu and bare Cu foils were added into wells respectively. To test the toxic effect of Cu^{2+} ion, 10 μl of Cu^{2+} ion solution in media was added to each new well with 3 ml of the lymphocyte suspension to get final ion concentration of 6.6×10^{-3} mM as a toxic source for T-cell activation. As the standard positive control, PMA (25 ng/ml) and ionomycin (2.5 $\mu\text{g}/\text{ml}$) were used to stimulate cell proliferation



as a means of comparison for other wells. Untreated wells were used as negative control. Each sample treatment was conducted in triplicate. After incubation for 1 day or 2 days in a humidified CO₂ incubator at 37°C, MTT tests were conducted to measure the number of lymphocytes.

In vivo experiment. The protocol was approved by the Purdue University Animal Care and Use Committee, and was performed in accordance with guidelines. Adult female Long-Evans rats (~300 g) were anesthetized by 90 mg/kg ketamine and 5 mg/kg xylazine. Skin and muscle was surgically opened by layer at T10 spine. After the exposure of spine, a piece of graphene coated Cu foil with size of 0.5 cm × 1.3 cm was implanted into the rat by the left side of the spine. Then the muscles and skin were closed in layers, and the rat was placed on a heating pad to maintain its body temperature until it awoke. The procedure was performed on three rats. A piece of bare Cu foil with the identical size was implanted into other three rats for comparison following the same procedure (Fig. S4 in supplementary information). The analgesic buprenorphine (0.05–0.10 mg/kg) was administered every 12 h through subcutaneous injection for the first 3 days post-surgery for post-operation pain management. To monitor concentration of Cu²⁺ ions, blood was extracted via jugular vein at 6 h, 12 h, 24 h, and up to 17 days after the implantation for ICP-MS analysis. Blood extracted from rats before the implantation procedure was used as control.

- Haddad, F. S. *et al.* Metal-on-metal bearings. *J. Bone Joint Surg. (Br.)* **93-B**, 572–579 (2011).
- Patterson, F. P. & Brown, C. S. The McKee-Farrar Total Hip Replacement Preliminary Results and Complications of 368 Operations Performed in Five General Hospitals. *J. Bone Joint Surg. (Am.)* **54**, 257–275 (1972).
- Korovessis, P., Petsinis, G., Repanti, M. & Repantis, T. Metallosis After Contemporary Metal-on-Metal Total Hip Arthroplasty Five to Nine-Year Follow-up. *J. Bone Joint Surg. (Am.)* **88**, 1183–1191 (2006).
- Kaw, M., Singh, S., Gagreja, H. & Azad, P. Role of self-expandable metal stents in the palliation of malignant duodenal obstruction. *Surg. Endosc.* **17**, 646–650 (2003).
- Baron, T. H. Expandable Metal Stents for the Treatment of Cancerous Obstruction of the Gastrointestinal Tract. *New Engl. J. Med.* **344**, 1681–1687 (2001).
- Cortizo, M., de Mele, M. & Cortizo, A. Metallic dental material biocompatibility in osteoblastlike cells. *Biol. Trace Elem. Res.* **100**, 151–168 (2004).
- Craig, R. G. & Powers, J. M. (eds.) *Restorative Dental Materials*, Edn. 11th. (Mosby Inc, 2002).
- Tondato, F. *et al.* Radiotherapy-induced pacemaker and implantable cardioverter defibrillator malfunction. *Expert Rev. Med. Devices* **6**, 243–249 (2009).
- Ishii, K. *et al.* Pacemaker Contact Dermatitis: The Effective Use of a Polytetrafluoroethylene Sheet. *Pacing Clin. Electrophysiol.* **29**, 1299–1302 (2006).
- Schmidt, C., Ignatius, A. A. & Claes, L. E. Proliferation and differentiation parameters of human osteoblasts on titanium and steel surfaces. *J. Biomed. Mater. Res.* **54**, 209–215 (2001).
- Kurtz, S. M., Muratoglu, O. K., Evans, M. & Edidin, A. A. Advances in the processing, sterilization, and crosslinking of ultra-high molecular weight polyethylene for total joint arthroplasty. *Biomaterials* **20**, 1659–1688 (1999).
- Davis, J. R. (ed.) *Handbook of Materials for Medical Devices*, Edn. 1st. (ASM International, 2003).
- Atwood, R. C., Lee, P. D. & Curtis, R. V. Modeling the surface contamination of dental titanium investment castings. *Dent. Mater.* **21**, 178–186 (2005).
- Caicedo, M. S., Pennekamp, P. H., McAllister, K., Jacobs, J. J. & Hallab, N. J. Soluble ions more than particulate cobalt-alloy implant debris induce monocyte costimulatory molecule expression and release of proinflammatory cytokines critical to metal-induced lymphocyte reactivity. *J. Biomed. Mater. Res. A* **93A**, 1312–1321 (2010).
- Romesburg, J. W., Wasserman, P. L. & Schoppe, C. H. Metallosis and Metal-Induced Synovitis Following Total Knee Arthroplasty: Review of Radiographic and CT Findings. (2010).
- Jacobs, J. J. & Hallab, N. J. Loosening and Osteolysis Associated with Metal-on-Metal Bearings: A Local Effect of Metal Hypersensitivity? *J. Bone Joint Surg. (Am.)* **88**, 1171–1172 (2006).
- Jacobs, J. J., Gilbert, J. L. & Urban, R. M. Current Concepts Review - Corrosion of Metal Orthopaedic Implants*. *J. Bone Joint Surg.* **80**, 268–282 (1998).
- Hunter, G., Dickinson, J., Herb, B. & Graham, R. in *Titanium, Niobium, Zirconium and Tantalum for Medical and Surgical Applications*. (eds. Zardiackas, L. D., Kraay, M. J. & Freese, H. L.) 16–29 (ASTM International, Ann Arbor, MI; 2006).
- Hobbs, L. W., Rosen, V. B., Mangin, S. P., Treska, M. & Hunter, G. Oxidation Microstructures and Interfaces in the Oxidized Zirconium Knee. *Int. J. Appl. Ceram. Technol.* **2**, 221–246 (2005).
- Desjardins, J. D., Burnikel, B. & LaBerge, M. UHMWPE wear against roughened oxidized zirconium and CoCr femoral knee components during force-controlled simulation. *Wear* **264**, 245–256 (2008).
- Yang, L., Sheldon, B. W. & Webster, T. J. Orthopedic nano diamond coatings: Control of surface properties and their impact on osteoblast adhesion and proliferation. *J. Biomed. Mater. Res. A* **91A**, 548–556 (2009).
- Pecheva, E. *et al.* Advanced Materials for Metal Implant Coatings. *J. Optoelectron. Adv. Mater.* **11**, 1323–1326 (2009).
- Nayak, T. R. *et al.* Graphene for Controlled and Accelerated Osteogenic Differentiation of Human Mesenchymal Stem Cells. *ACS Nano* **5**, 4670–4678 (2011).
- Bunch, J. S. *et al.* Impermeable Atomic Membranes from Graphene Sheets. *Nano Lett.* **8**, 2458–2462 (2008).
- Cho, J. *et al.* Atomic-Scale Investigation of Graphene Grown on Cu Foil and the Effects of Thermal Annealing. *ACS Nano* **5**, 3607–3613 (2011).
- Chen, S. *et al.* Oxidation Resistance of Graphene-Coated Cu and Cu/Ni Alloy. *ACS Nano* **5**, 1321–1327 (2011).
- Li, X. *et al.* Large-Area Synthesis of High-Quality and Uniform Graphene Films on Copper Foils. *Science* **324**, 1312–1314 (2009).
- Prasai, D., Tuberquia, J. C., Harl, R. R., Jennings, G. K. & Bolotin, K. I. Graphene: Corrosion-Inhibiting Coating. *ACS Nano* **6**, 1102–1108 (2012).
- Kirkland, N. T., Schiller, T., Medhekar, N. & Birbilis, N. Exploring graphene as a corrosion protection barrier. *Corros. Sci.* **56**, 1–4 (2012).
- Podila, R., Moore, T., Alexis, F. & Rao, A. M. Graphene coatings for enhanced hemo-compatibility of nitinol stents. *R. Soc. Chem. Adv.* **3**, 1660–1665 (2013).
- Podila, R., Moore, T., Alexis, F. & Rao, A. Graphene Coatings for Biomedical Implants. e50276 (2013).
- Neuhauser, E. F., Loehr, R. C., Milligan, D. L. & Malecki, M. R. Toxicity of metals to the earthworm *Eisenia fetida*. *Biol. Fert. Soils* **1**, 149–152 (1985).
- Li, J., Chung, T.-F., Chen, Y. P. & Cheng, G. J. Nanoscale Strainability of Graphene by Laser Shock-Induced Three-Dimensional Shaping. *Nano Lett.* **12**, 4577–4583 (2012).
- Cao, B. *et al.* Concentration-dependent cytotoxicity of copper ions on mouse fibroblasts in vitro: effects of copper ion release from TCu380A vs TCu220C intra-uterine devices. *Biomed. Microdevices* **14**, 709–720 (2012).
- Lee, S., Lee, K. & Zhong, Z. Wafer Scale Homogeneous Bilayer Graphene Films by Chemical Vapor Deposition. *Nano Lett.* **10**, 4702–4707 (2010).
- Koenig, S. P., Boddeti, N. G., Dunn, M. L. & Bunch, J. S. Ultrastrong adhesion of graphene membranes. *Nat. Nano.* **6**, 543–546 (2011).
- Cortizo, M. & Lorenzo de Mele, M. Cytotoxicity of copper ions released from metal. *Biol. Trace Elem. Res.* **102**, 129–141 (2004).
- Grillo, C. A., Reigosa, M. A. & Lorenzo de Mele, M. F. Effects of copper ions released from metallic copper on CHO-K1 cells. *Mutat. Res-Gen. Tox. En.* **672**, 45–50 (2009).
- Lagadic-Gossmann, D., Huc, L. & Lecreur, V. Alterations of intracellular pH homeostasis in apoptosis: origins and roles. *Cell Death Differ* **11**, 953–961 (2004).
- Barry, M. A. & Eastman, A. Endonuclease activation during apoptosis: The role of cytosolic Ca²⁺ and pH. *Biochem. Biophys. Res. Commun.* **186**, 782–789 (1992).
- Wlasny, I. *et al.* Role of graphene defects in corrosion of graphene-coated Cu(111) surface. *Appl. Phys. Lett.* **102**, 111601 (2013).
- Caprioli, F., Decker, F., Marrani, A. G., Beccari, M. & Castro, V. D. Copper protection by self-assembled monolayers of aromatic thiols in alkaline solutions. *Phys. Chem. Chem. Phys.* **12**, 9230–9238 (2010).
- Lusk, A. T. & Jennings, G. K. Characterization of Self-Assembled Monolayers Formed from Sodium S-Alkyl Thiosulfates on Copper. *Langmuir* **17**, 7830–7836 (2001).
- Munday, R. Toxicity of thiols and disulphides: Involvement of free-radical species. *Free Radic. Biol. Med.* **7**, 659–673 (1989).
- Sung, M. M. & Kim, Y. Self-Assembled Monolayers of Alkanethiols on Clean Copper Surfaces. *Bull. Korean Chem. Soc.* **22**, 5 (2001).
- Clinical immunology. Report of the committee on clinical immunology of the international union of immunological societies (IUIS) Background and aims. *Eur. J. Immunol.* **6**, 231–234 (1976).
- Klein, R., Schwenk, M., Heinrich-Ramm, R. & Templeton, D. M. Diagnostic relevance of the lymphocyte transformation test for sensitization to beryllium and other metals (IUPAC Technical Report). *Pure Appl. Chem.* **76**, 1269–1281 (2004).
- Lindemann, M., Rietschel, F., Zabel, M. & Grosse-Wilde, H. Detection of chromium allergy by cellular in vitro methods. *Clin. Exp. Allergy* **38**, 1468–1475 (2008).
- Belouski, S. S. *et al.* Utility of lyophilized PMA and ionomycin to stimulate lymphocytes in whole blood for immunological assays. *Cytometry B Clin. Cytom.* **78B**, 59–64 (2010).
- Verma, A. *et al.* Evaluation of the MTT lymphocyte proliferation assay for the diagnosis of neurocysticercosis. *J. Microbiol. Methods* **81**, 175–178 (2010).
- Hallab, N. J., Caicedo, M. S., Finnegan, A. & Jacobs, J. J. Th1 type lymphocyte reactivity to metals in patients with total hip arthroplasty. *J. Orthop. Surg. Res.* **3**, 11 (2008).
- Puig, S. & Thiele, D. J. Molecular mechanisms of copper uptake and distribution. *Curr. Opin. Chem. Biol.* **6**, 171–180 (2002).
- Cabrera, A. *et al.* Copper binding components of blood plasma and organs, and their responses to influx of large doses of 65Cu, in the mouse. *Biomaterials* **21**, 525–543 (2008).

Acknowledgments

We acknowledge Greg Cresswell, Hsing-Hui Wang and Renee E Wenig for their help with collecting lymphocytes from mouse spleens, Wei Wu and Junjie Li for their help with collecting mouse spleens and the MTT instrument. C. Yang thanks support from Purdue Research Foundation. Z. Zhong thanks support from National Science Foundation Scalable



Nanomanufacturing Program (DMR-1120187). Y.P. Chen acknowledges that the synthesis of SLG was supported in part by NSF (DMR 0847638) and DTRA (HDTRA1-09-1-0047).

Author contributions

W.Z. and C.Y. designed this work and wrote the paper. W.Z. performed the major part of the experiments. S.L. and K.L.M. helped to conduct chemical and cellular experiment. T.F.C., S.L., K.L., Z.Z. and Y.P.C. helped to prepare graphene samples. S.A.C. and T.L.R. helped to conduct lymphocyte transformation test.

Additional information

Supplementary information accompanies this paper at <http://www.nature.com/scientificreports>

Competing financial interests: The authors declare no competing financial interests.

How to cite this article: Zhang, W.X. *et al.* Use of graphene as protection film in biological environments. *Sci. Rep.* 4, 4097; DOI:10.1038/srep04097 (2014).



This work is licensed under a Creative Commons Attribution-NonCommercial-NoDerivs 3.0 Unported license. To view a copy of this license, visit <http://creativecommons.org/licenses/by-nc-nd/3.0>